

Photoplethysmography based stratification of blood pressure using multi information fusion artificial neural network

Dingliang Wang¹, Xuezhi Yang², Xuenan Liu¹, Shuai Fang¹, Likun Ma³, Longwei Li³

¹School of Computer and Information, Hefei University of Technology, Hefei, China

²School of Software, Hefei University of Technology, Hefei, China

³The First Affiliated Hospital of University of Science and Technology of China, Hefei, China

wdlwshcjf@163.com, xzyang@hfut.edu.cn, xuenanliu@mail.hfut.edu.cn,

fangshuai@hfut.edu.cn, lkma119@163.com, llw3831@163.com

Abstract

Regular monitoring of blood pressure (BP) is an effective way to prevent cardiovascular diseases, especially for elderly people. At present, BP measurement mainly relies on cuff-based devices which are inconvenient for users and may cause discomfort. Therefore, many new approaches have been proposed to achieve cuff-less BP detection in recent years. However, the accuracy of the existing approaches still needs to be improved. In this study, holistic-based PPG and its first and second derivative features are extracted and a new multi information fusion artificial neural network (MIF-ANN) is designed to effectively fuse and exploit multiple input data. Experimental results on a public database which contains 12000 subjects show that the proposed network can model the relation between Photoplethysmography (PPG) and BP well, achieving averagely accuracy of 91.33% for 5-category BP stratification. Additionally, this study verified that multi information fusion based on meticulously designed network plays an important role in improving the accuracy of BP detection.

1. Introduction

Blood pressure (BP) is an important physiological parameter for assessing cardiovascular health which refers to the lateral pressure acts on the vessel wall when the blood flows in the blood vessel. Abnormal BP increases the risk of cardiovascular and cerebrovascular diseases (CCVD) such as cerebral apoplexy, atherosclerosis and heart failure [2, 10]. Therefore, early detection and control of abnormal BP like hypertension and hypotension could effectively prevent CCVD. At present, cuff-based BP measurement devices have been widely used in hospital which are not convenient and comfortable for users; this shortcoming greatly limited the wide application of BP detection, especially for daily con-

tinuous monitoring.

In the past decades, many new approaches have been proposed to achieve cuff-less BP measurement. Among them, pulse transit time (PTT) based method was thoroughly verified by researchers. In 1981, Geddes *et al.* initially analyzed the relationship between BP and PTT, and found a good linear correlation between the two [6]. In 2001, Chan *et al.* used electrocardiograph (ECG) and photoplethysmography (PPG) signals to calculate PTT from which the BP value was estimated with a calibration for each subject [3]. They adopted the mean error (ME) between predicted BP and ground-truth BP as the evaluation standard and achieved ME of 7.5 mmHg for systolic blood pressure (SBP) and 4.1 mmHg for diastolic blood pressure (DBP). In 2017, Kachuee *et al.* proposed a calibration-free BP estimation method based on PTT [14]. Their best results were obtained using adaptive boosting (AdaBoost), achieving mean absolute error (MAE) of 11.17 mmHg for SBP and 5.35 mmHg for DBP. Afterwards, the research on deep learning started to rise, and in 2018, Su *et al.* used PTT alongside other features as the input of a recurrent neural network (RNN) to model the relation between PTT and BP [22]. They achieved root mean square error (RMSE) of 3.90 and 2.66 mmHg for SBP and DBP respectively. Although the effectiveness of PTT based method was verified repeatedly, its shortcomings are also obvious. Firstly, the calculation of PTT requires two sensors to synchronously collect physiological signals such as ECG and PPG, which increases the complexity of BP detection. Besides, the time delay of the collected signals from the two sensors must be accurately calculated, which requires precise synchronization and a lot of efforts for signal preprocessing.

Due to the aforementioned reasons, this study focuses on BP measurement using single PPG signal. As shown in Figure 1, the features of pulse wave PPG signal such as cycle length, amplitude and morphological characteristics

are closely related to cardiovascular status, for example, the gradient of rapid ejection period is thought to be positively correlated with systolic blood pressure, and the amplitude ratio of systolic peak to diastolic peak is associated with arteriosclerosis [19, 18, 26, 11]. In 2013, Kurylyak *et al.* extracted 21 features from a PPG cycle and these features were then fed into an artificial neural network (ANN) to estimate BP [16]. Their BP prediction results are good but the dataset they used is too small. Liang *et al.* used the continuous wavelet transform (CWT) to extract temporal-spectrum PPG features as the input of a convolutional neural network (CNN) to achieve BP stratification [17]. They divided BP into three categories: normotension, prehypertension and hypertension, realizing accuracy of 80.52%, 92.55%, and 82.95% for the three classification respectively. Wang *et al.* compared three methods for BP estimation based on MIMIC [20, 12] database: linear regression, support vector machine (SVM) and ANN, and their best results were obtained using ANN with MAE of 4.02 ± 2.79 mmHg for SBP and 2.27 ± 1.82 mmHg for DBP [24]. The shortcoming is that their experiments were conducted on only 90 patients. Dey *et al.* utilized the time and frequency domain features extracted from PPG, velocity plethysmography (VPG - the first derivative of PPG) and acceleration plethysmography (APG - the second derivative of PPG) signals for BP estimation based on Lasso regression and achieved MAE of 6.9 mmHg and 5.0 mmHg for SBP and DBP respectively [5]. But their experiments were based on self-collected data of 205 volunteers and they have not explained whether their data contains hypotension or hypertension individuals. Visvanathan *et al.* combines time domain PPG features with personal information such as age, height and weight to classify BP levels using SVM and achieved a high accuracy of 100% [23], but their method was verified on only 32 cases and their smartphone dataset cannot be publicly accessed. In 2019, Somayyeh *et al.* proposed a whole-based method to extract PPG features which significantly improved the anti-noise performance [21], but their BP estimation accuracy is not that ideal which just reached grade C according to the British Hypertension Society (BHS) standard. Based on the above analysis, it is obvious that combining artificial extracted features with machine learning or deep learning algorithms is the main research direction of PPG-based BP measurement and the detection accuracy of BP still needs to be improved.

In this article, a new method is proposed to achieve 5-category BP stratification as it is sufficient to judge cardiovascular status by BP levels rather than precise BP values. The method uses holistic-based features extracted from PPG, VPG and APG as the input of a specially designed neural network, which are less sensitive to noise compared with non-holistic-based features. The main contributions of this article are as follows:

1. The experiments are conducted on a large, precisely specified database which contains 12000 samples with available arterial blood pressure (ABP) and PPG recorded simultaneously at 125 Hz for each sample. The large database conduces to train a good general model using machine learning or deep learning algorithms;
2. Holistic-based features of both time and frequency domain are extracted from PPG, VPG and APG, which improved the robustness to noise, and therefore can promote PPG-based cuff-less BP measurement moving towards practical application using consume-level cameras;
3. A new artificial neural network structure is designed to realize the fusion and effective utilization of multiple information. Furthermore, the neural network architecture can be flexibly adjusted to meet the requirements of different tasks. The details of the designed neural network will be described in the later sections.

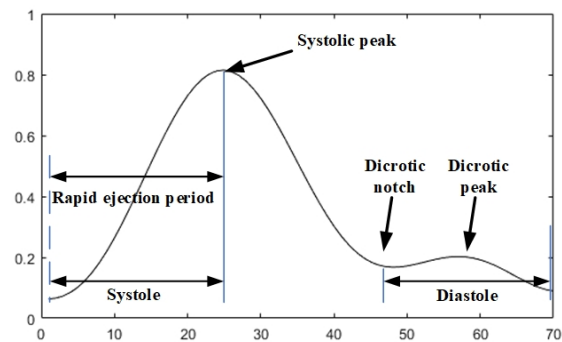


Figure 1. An example of single cycle pulse wave signal.

2. Method

The overall framework of the proposed method is shown in Figure 2 where both the arterial blood pressure (ABP) and PPG signals are from a public UCI machine learning blood pressure (UCI-ML-BP) database which is available online at <http://archive.ics.uci.edu/ml/datasets/Cuff-Less+Blood+Pressure+Estimation> [13, 8]. This section will explain the proposed method in detail to show how it works.

2.1. Generate BP category labels

The ABP signals in UCI-ML-BP database are used to extract SBP and DBP so that BP category labels can be determined on the basis. The extraction method is shown in Figure 3. When the ABP signal is of high quality, SBP and DBP can be obtained by a simple peak detection algorithm with averaged peak values corresponds to SBP and averaged valley values corresponds to DBP. But in most cases, the ABP signal is not that ideal and exists one or more irregular interference which may result from the motions in

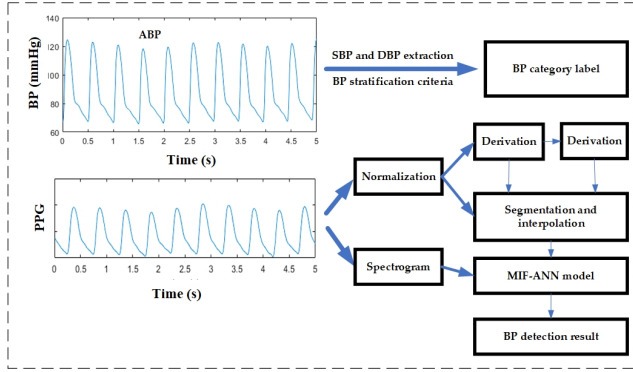


Figure 2. The overall framework of the proposed BP stratification method.

the process of BP measurement. So, an abnormal detection method is applied to find and discard abnormal peak and valley values. First, the standard deviation and mean of peak (valley) values are calculated, then compute the deviation between each peak (valley) value and the mean. If the absolute value of a deviation is larger than two times of standard deviation, the corresponding peak (valley) will be discarded as noise. After the above procedures, all SBP and

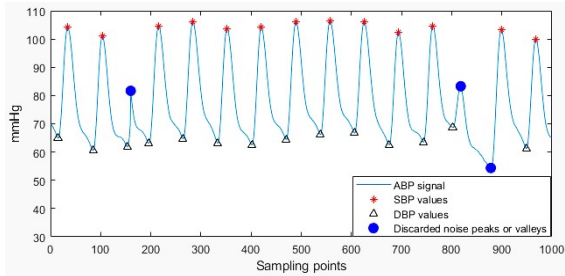


Figure 3. SBP and DBP extraction from ABP signal.

DBP of total 12000 records in the UCI-ML-BP database are obtained and Figure 4 is the distribution of the extracted SBP and DBP. It is clear that the database covers all kinds of BP categories such as hypotension, normotension, prehypertension and hypertension with SBP between 69 and 196 mmHg while DBP between 50 and 163 mmHg. Given SBP and DBP, BP category labels can be determined now. According to the seventh report of the Joint National Committee on Prevention, Detection, Evaluation, and Treatment of High Blood Pressure (JNC7), BP can be divided into four categories: normotension, prehypertension, stage 1 hypertension and stage 2 hypertension [4]. This study added one hypotension category on the basis of JNC7, and Table 1 is the detailed stratification criteria. The obtained BP category labels will be used as the prediction result of artificial neural network (ANN).

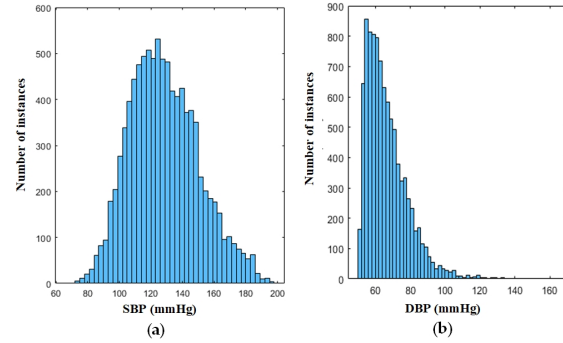


Figure 4. Histogram of extracted SBP and DBP from UCI-ML-BP database: (a) Distribution of systolic blood pressure; (b) Distribution of diastolic blood pressure.

Table 1. Stratification criteria of blood pressure.

BP category	SBP (mmHg)	operator	DBP (mmHg)
hypotension	<90	and	<60
normotension	90~119	or	60~79
prehypertension	120~139	or	80~89
stage 1 hypertension	140~159	or	90~99
stage 2 hypertension	≥ 160	or	≥ 100

2.2. Holistic-based features extraction

Other algorithms usually detect BP based on the feature values calculated from the feature points of a PPG signal. These features are highly related to the form of the PPG signal and a slight noise in PPG signal may influence the extracted feature values significantly. The proposed holistic-based method uses continuous values of the original signal for BP stratification. Compared to non-holistic-based methods, our method is less sensitive to noise and therefore can tolerate stronger interference. The extracted holistic-based

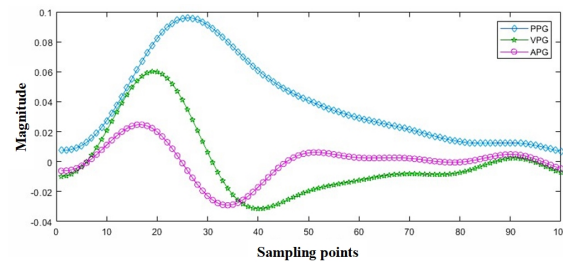


Figure 5. Single period PPG waveform and its derivatives after segmentation.

features contain PPG and its derivatives as the derivatives also carry valuable information related to cardiovascular circulation [25]. Firstly, the PPG signal is normalized and its first-order derivation (VPG) and second-order derivation

(APG) are calculated. Then, the single-cycle segmentation of PPG, VPG and APG signal is performed. Figure 5 shows the segmented single period PPG, VPG and APG waveforms.

Afterwards, an interpolation procedure is performed to make sure that all feature vectors extracted from UCI-ML-BP database are the same length. The sampling rate of PPG signals is 125 Hz and according to our calculation from PPG, the minimum and maximum heart rate in UCI-ML-BP database are 48 and 125 beats per minute (bpm), respectively. So, it is sufficient to record all points of a single cycle for all PPG signals if the length of feature vectors is larger than 156. In this study, the length of feature vectors for PPG, VPG and APG is set to 200. The interpolation approach is simple, that is, padding with zeros in the end of the original single period PPG, VPG and APG waveforms. Figure 6 shows an example of the obtained feature vectors after padding zeros.

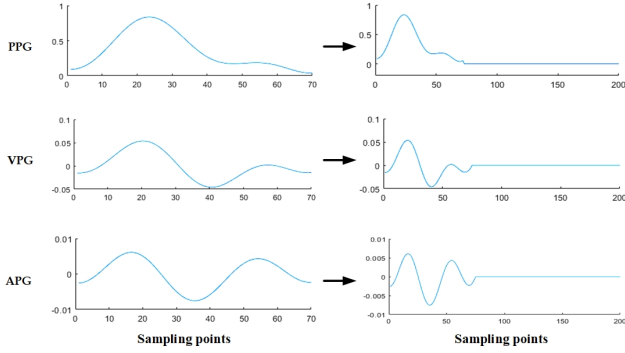


Figure 6. Extracted holistic-based feature vectors from PPG, VPG and APG. All feature vectors are interpolated to equal length.

Apart from the above time domain features, temporal-spectrum information is further extracted for training artificial neural network and improving BP stratification accuracy. Generalized Morse wavelet (GMW) is an accurate analytic wavelet for extracting temporal-spectrum features, which uses β and γ two parameters to adjust its waveform, its frequency domain representation is:

$$\Psi_{\beta,\gamma}(\omega) = 2H(\omega)\left(\frac{e^\gamma}{\beta}\right)^{\frac{\beta}{\gamma}}\omega^\beta \exp(-\omega^\gamma) \quad (1)$$

where $H(\omega)$ is Heaviside step function, e is Euler number, β and γ are two variable parameters which can be controlled to compare with original PPG signal and obtain wavelet coefficients. Compared with Morse wavelet which is only approximated analytic, GMW is completely analytic and is capable of more effective extraction of local features in the pulse wave. Thus, GMW is chosen as the base of continuous wavelet transform (CWT). Figure 7 shows an example of extracted temporal-spectrum graph.

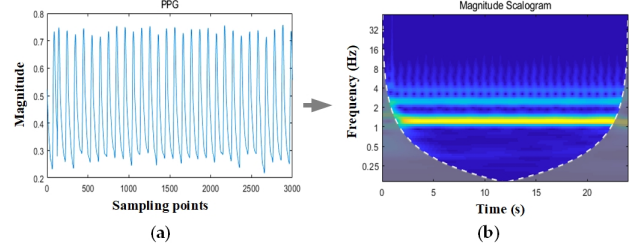


Figure 7. Extracting temporal-spectrum features using CWT: (a) Original PPG waveform of 24 seconds; (b) Extracted temporal-spectrum graph using generalized Morse wavelet.

2.3. Neural network design and hyperparameters

The performance of a single neural network classifier depends heavily on the choice of network parameters, so it is very difficult to design an optimal neural network classifier for a complex classification task. To solve this problem, the multi information fusion artificial neural network (MIF-ANN) is designed to improve BP stratification accuracy which combines multiple ANN classifiers for processing different input data respectively. Figure 8 is the schematic structure of MIF-ANN.

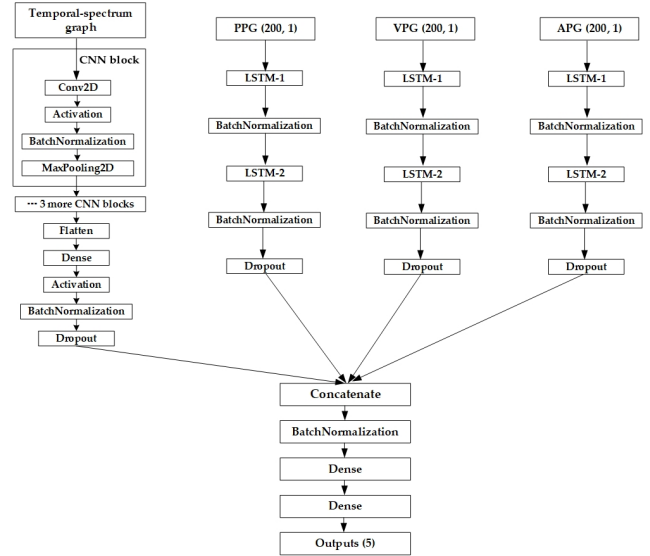


Figure 8. Overall architecture of the proposed multi information fusion artificial neural network.

As shown in Figure 8, the temporal-spectrum graph is used as the input of a convolutional neural network (CNN) which contains 4 CNN blocks. Each CNN block consists of convolutional layer, activation layer, batch normalization and max pooling. As for activation layer, ReLU is adopted as the activation function to accelerate the training process. Batch normalization is used to reduce covariate shift and

mitigate vanishing gradient problem. Max pooling layer is used for dimensionality reduction. Afterwards, the CNN outputs are flattened and passed to a dense (fully connected) layer [15].

The single period PPG, VPG and APG feature vectors are fed to 3 long short-term memory (LSTM) networks, respectively. LSTM is an improvement of recurrent neural network (RNN). RNN is capable of processing short time sequences, but when the data is long, gradient disappearance and gradient explosion problem will occur. Therefore, LSTM is proposed which achieved long dependence processing by combining forgetting gate, input gate and output gate [9, 7].

The outputs of four networks are then concatenated and passed into a multi-layer perceptron (MLP) model which consists of two dense layers and one output layer. The final output layer uses softmax function shown in (2) to produce predicted result of BP categories.

$$S_i = \frac{e^{y_i}}{\sum_{j=1}^k e^{y_j}} \quad (2)$$

where k is the number of output elements, y_i is the i_{th} output of the final dense layer, and the sum of S_i is 1. Apparently, the softmax function maps the outputs of multiple neurons into (0,1) interval, and the outputs of softmax can be regarded as the probability of belonging to each category.

The MIF-ANN were trained with learning rate of 0.001 and batch size of 256. The maximum number of training epochs was set to 400, with stopping performed if the results of 15 consecutive trainings have no improvement. The categorical cross entropy loss function shown in (3) is adopted to optimize the network:

$$loss = -\frac{1}{n} \sum_{i=1}^n [y_i \ln z_i + (1 - y_i) \ln (1 - z_i)] \quad (3)$$

where n is the number of categories (equal to the number of output elements), y is the expected output, z is the actual output of neural network which can be formulated as:

$$z = \mathbf{w}^T \mathbf{x} + \mathbf{b} \quad (4)$$

here, \mathbf{w} is the matrix of MIF-ANN weight vectors, \mathbf{x} is the input vector, \mathbf{b} is the bias vector. Apparently, the value of categorical cross entropy loss function is close to 0 when actual output is close to expected output.

3. Results

3.1. Experimental setup

In order to evaluate the performance of the proposed method, the public UCI-ML-BP database is used as our ABP and PPG data source so that all researchers who

would like to do further comparison fairly could access this database easily. UCI-BP database contains 12000 data records gathered at several hospitals and each record consists of synchronously collected PPG and ABP signals with sampling frequency of 125 Hz and time length of 24 seconds [8]. All the modeling, training and testing were based on tensorflow-gpu-1.11.0 and keras-2.2.5 deep learning toolbox using python3.6 environment [1]. Considering the amount of data and the extreme computational complexity when training the MIF-ANN model, a high-performance workstation is used which contains 128GB physical memory and NVIDIA Tesla P100 16GB GPU memory.

3.2. Experimental results

The experiments were conducted using K fold cross validation (KF-CV), which improved the robustness in training a good general model. KF-CV method is simple but effective: Suppose the dataset has N samples, divide these samples into K parts, $K-1$ parts are used for training the classifier, and the remain one part is used for validation. After K times of iteration, all samples have been trained and validated. Figure 9 shows the loss curve and accuracy curve of the training process of the final iteration where the training accuracy converges to about 96%. Note that the K value in the experiment is set to 10.

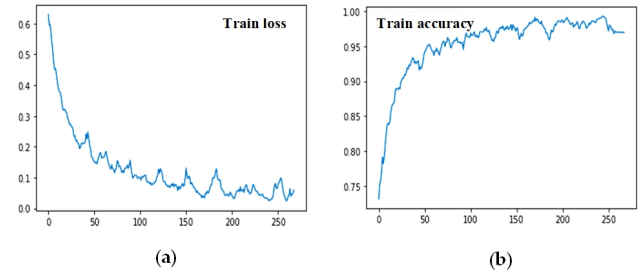


Figure 9. Training curves of MIF-ANN network: (a) The loss curve; (b) The accuracy curve.

The test result of BP stratification is shown in Table 2 where other well-established methods using single PPG signal are compared. Note that most of the compared methods are to achieve BP estimation, and therefore, the BP estimation result is further utilized to determine BP category according to the stratification criteria shown in Table 1. Experimental results show that the proposed method outperforms other methods in terms of BP stratification with average test accuracy of 91.33%. The test accuracy is similar to training accuracy which means the MIF-ANN model is not overfitting. The correct rate (CR) of recognizing hypotension, normotension, prehypertension, stage 1 hypertension and stage 2 hypertension are 89.67%, 94.35%, 90.44%, 85.21% and 91.50% respectively which verified that it is feasible to evaluate BP on a large dataset using single PPG signal. This is a

Table 2. Comparison of well-established methods based on UCI-ML-BP database using single PPG signal. Note, LT, NT, PHT, HT1 and HT2 represent hypotension, normotension, prehypertension, stage 1 hypertension and stage 2 hypertension respectively. CR stands for the correct rate of recognizing corresponding BP category.

Author	Used methods	CR of LT	CR of NT	CR of PHT	CR of HT1	CR of HT2	Average accuracy
Liang <i>et al.</i> [17]	Temporal-spectrum PPG features; CNN	77.65%	83.08%	88.07%	82.50%	84.26%	82.41%
Wang <i>et al.</i> [24]	Time and frequency domain PPG features; fully connected ANN	81.24%	88.53%	84.36%	87.12%	89.13%	86.52%
Dey <i>et al.</i> [5]	Time and frequency domain PPG features; Lasso regression	62.32%	79.96%	79.57%	60.02%	62.65%	71.43%
Visvanathan <i>et al.</i> [23]	Time domain PPG features; SVM	61.33%	81.40%	70.28%	62.47%	54.72%	72.54%
Somayyeh <i>et al.</i> [21]	Time domain holistic-based PPG features; non-linear regression	86.54%	86.05%	89.75%	81.20%	84.77%	83.95%
Our method	Holistic-based time and frequency domain PPG features; MIF-ANN	89.67%	94.35%	90.44%	85.21%	91.50%	91.33%

big step for pushing PPG-based cuff-less BP measurement from theoretical research to practical application.

Furthermore, the accuracy of BP stratification using single PPG feature and multiple PPG features are compared to verify whether the fusion of multi information is reasonable and effective. The comparison result is shown in Table 3 which validated that the accuracy of BP stratification can be significantly improved by combining multiple information from time and frequency domain PPG signal and its first and second derivatives using the specially designed MIF-ANN model.

Table 3. Comparison of BP stratification results using single PPG feature and multiple PPG features.

Input features	Model	Average accuracy of recognizing BP categories
PPG	LSTM	79.40%
VPG	LSTM	81.95%
APG	LSTM	61.78%
Temporal-spectrum graph	CNN	83.25%
PPG + VPG + APG + temporal-spectrum graph	MIF-ANN (3 LSTMs +1 CNN)	91.33%

4. Conclusions

A new PPG-based BP stratification approach is proposed in this study which combines time and frequency domain features of PPG and its first and second derivatives to improve BP detection accuracy. Correspondingly, the MIF-ANN model which consists of one CNN and three LSTM networks is designed to achieve the effective fusion of multiple input features. Our experiments are based on a public large database for the purpose of training a good generalized BP stratification model, and the experimental results show that the proposed method outperforms other well-established methods with average classification accuracy of 91.33% for 5-category BP stratification, which is a big step for accelerating cuff-less continuous BP monitoring moving towards practical application.

The extracted features are holistic-based which improved the tolerance for noise of PPG signal compared to other non-holistic-based features, and the newly designed MIF-ANN model can be easily expanded to process more inputs while all the input data are trained independently. Furthermore, the proposed method is verified on a public database so that other researchers who would like to do further comparison can access the data easily. The main focus of our future research is on whether the trained MIF-ANN model is suitable for the pulse wave collected by ourselves using mobile phone cameras or other PPG sensors. Besides, individual information such as age, gender and height should be added to our model for personalized calibration in future work.

Acknowledgement

This research is funded by “the Key Technology and System of Cardiovascular Disease Detection Based on Video Pulse Wave” under the Major Science and Technology Projects of Anhui Province with grant No. 201903c08020010.

References

- [1] M. Abadi, P. Barham, and J. Chen. Tensorflow: A system for large-scale machine learning. 2016. [5](#)
- [2] J. Allen. Photoplethysmography and its application in clinical physiological measurement. *Physiol. Meas.*, 28(3):1–22, 2007. [1](#)
- [3] K. W. Chan, k. hung, and Y. T. Zhang. Noninvasive and cuffless measurements of blood pressure for telemedicine. *In Proceedings of the 23rd Annual International Conference of the IEEE Engineering in Medicine and Biology Society*, pages 3592–3593, 2001. [1](#)
- [4] A. V. Chobanian, G. L. Bakris, H. R. Black, W. C. Cushman, L. A. Green, J. L. Izzo, and D. W. Jones. Seventh report of the joint national committee on prevention, detection, evaluation, and treatment of high blood pressure. *Hypertension*, 289(19):1206–1252, 2003. [3](#)
- [5] J. Dey, A. Gaurav, and V. N. Tiwari. Instabp: Cuff-less blood pressure monitoring on smartphone using single ppg sensor. *40th Annual International Conference of the IEEE Engineering in Medicine and Biology Society*, pages 5002–5005, 2018. [2](#), [6](#)
- [6] L. A. Geddes, M. H. Voelz, C. F. Babbs, J. D. Bourl, and W. A. Tacker. Pulse transit time as an indicator of arterial blood pressure. *Psychophysiology*, 18(1):71–74, 1981. [1](#)
- [7] F. A. Gers, J. Schmidhuber, and F. A. Cummins. Learning to forget: Continual prediction with lstm. *Neural Comput.*, 12(10):2451–2471, 2000. [5](#)
- [8] A. L. Goldberger, L. A. Amaral, L. Glass, J. M. Hausdorff, P. C. Ivanov, and R. G. Mark. Physiobank, physiotoolkit, and physionet: Components of a new research resource for complex physiologic signals. *Circulation*, 101, 2000. [2](#), [5](#)
- [9] S. Hochreiter and J. Schmidhuber. Long short-term memory. *Neural Comput.*, 9(8):1735–1780, 1997. [5](#)
- [10] C. Höcht. Blood pressure variability: prognostic value and therapeutic implications. *ISRN hypertension*, 2013. [1](#)
- [11] H. S. James, R. Stern, H. B. Jodi, E. K. Claudia, W. H. Erika, Y. Terry, and E. P. Paul. Relationships between sleep apnea, cardiovascular disease risk factors, and aortic pulse wave velocity over 18 years: the wisconsin sleep cohort. *Sleep and Breathing*, 20(2):813–817, 2016. [2](#)
- [12] A. E. Johnson, T. J. Pollard, L. Shen, H. L. Li-wei, M. Feng, M. Ghassemi, B. Moody, P. Szolovits, L. A. Celi, and R. G. Mark. MIMIC-III, a freely accessible critical care database. *Scientific Data*, 3, 2016. [2](#)
- [13] M. Kachuee, M. M. Kiani, H. Mohammadzade, and M. Shabany. Cuff-less high-accuracy calibration-free blood pressure estimation using pulse transit time. *IEEE International Symposium on Circuits and Systems*, pages 1006–1009, 2015. [2](#)
- [14] M. Kachuee, M. M. Kiani, H. Mohammadzade, and M. Shabany. Cuffless blood pressure estimation algorithms for continuous health-care monitoring. *IEEE Trans. Biomed. Eng.*, 64(4):859–869, 2017. [1](#)
- [15] A. Krizhevsky, I. Sutskever, and G. E. Hinton. Imagenet classification with deep convolutional neural networks. *In Proceedings of the Advances in Neural Information Processing Systems*, pages 1097–1105, 2012. [5](#)
- [16] Y. Kurylyak, F. Lamonaca, and D. Grimaldi. A neural network-based method for continuous blood pressure estimation from a ppg signal. *In Proceedings of the 2013 IEEE International Instrumentation and Measurement Technology Conference*, pages 280–283, 2013. [2](#)
- [17] Y. Liang, Z. Chen, R. Ward, and M. Elgendi. Photoplethysmography and deep learning: Enhancing hypertension risk stratification. *Biosensors*, 2018. [2](#), [6](#)
- [18] W. Liu, X. Fang, Q. Chen, Y. Li, and T. Li. Reliability analysis of an integrated device of ecg, ppg and pressure pulse wave for cardiovascular disease. *Microelectronics Reliability*, 87:183–187, 2018. [2](#)
- [19] I. Pavlidis, J. Dowdall, N. Sun, C. Puri, J. Fei, and M. Garbey. Interacting with human physiology. *Computer Vis. Image Understand*, 108(1):150–170, 2017. [2](#)
- [20] M. Saeed, M. Villarroel, A. T. Reisner, G. Clifford, L. W. Lehman, G. Moody, T. Heldt, T. H. Kyaw, B. Moody, and R. G. Mark. Multiparameter intelligent monitoring in intensive care ii: A public-access intensive care unit database. *Crit. Care Med.*, 39:952–960, 2011. [2](#)
- [21] M. S. Somayyeh, F. Mohammad, C. Mostafa, H. Mohammad, M. Maryam, and G. Yadollah. Blood pressure estimation from appropriate and inappropriate ppg signals using a whole-based method. *Biomedical Signal Processing and Control*, 47:196–206, 2019. [2](#), [6](#)
- [22] P. Su, X. R. Ding, Y. T. Zhang, J. Liu, F. Miao, and N. Zhao. Long-term blood pressure prediction with deep recurrent neural networks. *In Proceedings of the 2018 IEEE EMBS International Conference on Biomedical and Health Informatics*, pages 323–328, 2018. [1](#)
- [23] A. Visvanathan, A. Sinha, and A. Pal. Estimation of blood pressure levels from reflective photoplethysmograph using smart phones. *IEEE 13th International Conference on Bioinformatics and Bioengineering*, 2013. [2](#), [6](#)
- [24] L. Wang, W. Zhou, Y. Xing, and X. Zhou. A novel neural network model for blood pressure estimation using photoplethysmography without electrocardiogram. *Journal of Healthcare Engineering*, 2018:1–9, 2018. [2](#), [6](#)
- [25] K. Q. Yousef, U. Rubins, and A. Mafawez. Photoplethysmogram second derivative review: Analysis and applications. *Scientific research and essays*, 10(21):633–639, 2015. [3](#)
- [26] W. Zhong, K. J. Cruickshanks, C. R. Schubert, C. M. Carlsson, R. J. R. J. Chappell, B. E. Klein, R. Klein, and C. W. Acher. Pulse wave velocity and cognitive function in older adults. *Alzheimer Disease and Associated Disorders*, 28(1):44–49, 2014. [2](#)